JOURNAL OF MATERIALS SCIENCE 13 (1978) 202–207

Anelastic deformation and the friction stress of bone

W. BONFIELD, P. O'CONNOR*
Department of Materials, Queen Mary College, London, UK

The elastic and non-elastic tensile deformation characteristics of longitudinal bovine and rabbit compact bone specimens have been measured with a microstrain technique. For both types of specimen, limited elastic deformation was observed, with a microscopic yield stress (MYS) (the stress to produce a non-elastic strain of 2×10^{-6}) of $12 \pm 8\,MNm^{-2}$. Measurements of stress–strain behaviour during loading, unloading and recovery of residual non-elastic strain with time at zero stress, which were made for stress increments from the MYS to fracture, revealed a series of closed hysteresis loops. From these results, the non-elastic strain is attributed entirely to anelastic deformation and the concept of a friction stress (σ_F), which defines the onset of anelastic deformation, is introduced.

1. Introduction

Two types of yield behaviour have been identified in studies of the stress–strain behaviour of compact bone. At relatively high stress levels (50 to 90% of the ultimate tensile strength), non-elastic strain of $>10^{-3}$ has been observed [1–3] and generally attributed to the onset of plastic strain. For convenience, this yield stress will be subsequently referred to as the macroscopic yield stress. In contrast, the use of microstrain measuring techniques, (with a strain measurement sensitivity of 10^{-6}) resulted in the definition of a yield stress at much smaller stress levels (<1% of the ultimate tensile strength) [4–7], which was designated as the microscopic yield stress (MYS). It was established that the non-elastic strain associated with the MYS was recoverable with time after unloading to zero stress. Hence the non-elastic strain was completely anelastic (i.e. recoverable with time) and did not include any plastic (i.e. permanent) strain. In this paper, the non-elastic strain produced by constant strain rate tensile deformation is determined for stress increments from the MYS to the ultimate tensile strength and, for the specimens examined, is correlated entirely with anelastic behaviour. The concept of a friction stress (σ_F) which defines the onset of anelastic deformation, is introduced and derived from the energy loss in a hysteresis loop.

2. Experimental procedure

Longitudinally oriented specimens, with a rectangular cross-section of $\sim(1 \times 10^{-4})$ m $\times$ (2×10^{-4}) m, a gauge length of $\sim 3.7 \times 10^{-2}$ m and shoulder radius of curvature of 6.4×10^{-4} m, were machined (with the resultant temperature rise measured as $<1^\circ$ C) from 2 to 3 years bovine femur and tibia sections. Similarly shaped, but shorter gauge length ($\sim 1.5 \times 10^{-2}$ m), specimens were prepared from one-year rabbit femur and tibia sections. Each specimen was mechanically polished, inspected microscopically for surface cracks and accurately measured. With the exception of these operations, the specimens were stored (at -5° C), machined and also tested in Ringers solution. Full details of these procedures are given elsewhere [8].

Tensile tests were performed on an Instron testing machine at 25° C. Strain was measured from EA-06-031 DE-120 type micro resistance strain gauges on the specimen gauge length [6], which gave a strain resolution of 2×10^{-6} on a

*Now at Department of Pathology, University of Manchester.

© 1978 Chapman and Hall Ltd. Printed in Great Britain.

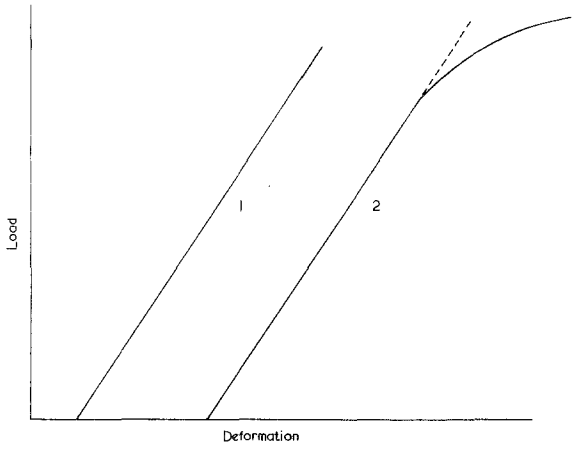

Figure 1 Schematic illustration of an Instron chart recording of Type 1 and Type 2 load-deformation behaviour to fracture.

Vishay–Ellis–20A digital meter, and stress was calculated from the load recorded on the Instron chart divided by the original cross-sectional area.

In the tensile tests, the specimen was loaded to a given stress value at a constant strain rate (between 2.25×10^{-6} and $2.25 \times 10^{-4}\ s^{-1}$), with the total strain measured at convenient intervals, and then unloaded at the same rate to zero stress. The value of any initial residual non-elastic strain at zero stress was noted, as was the subsequent recovery of the non-elastic strain with time. The specimen was allowed to recover completely to zero strain before any subsequent tests were performed. This procedure was repeated for a series of increasing stress levels, which for some specimens were continued until fracture occurred.

3. Results

3.1. Stress–total strain to fracture

The load-deformation behaviour to fracture at a constant strain rate recorded on the Instron testing machine chart was of two types, as illustrated in Fig. 1, with most specimens exhibiting Type 1 behaviour (an "apparent" linear elastic deformation) and some specimens Type 2 behaviour (with a significant departure from linearity prior to fracture). However direct measurement of total strain from the specimen gauge length, and with microstrain sensitivity, revealed that both Type 1 and Type 2 curves were in fact non-linear at stress levels from $\sim 10\,MNm^{-2}$ to fracture, as shown in Fig. 2 for Type 1 behaviour. The various aspects of deformation revealed in Fig. 2 are considered in the following sections.

3.2. Linear stress–total strain

Fig. 2 reveals that the initial stress–total strain curve was linear. It was demonstrated that the deformation was also elastic by performing load–unloading cycles within this region, which followed a straight line such as shown schematically as line (A) in Fig. 3. Any derivation of Young's modulus ($E = \sigma/\epsilon$) should obviously be made within the restricted limits of elastic behaviour ($\sigma < 20\,MNm^{-2}$, $\epsilon < 800 \times 10^{-6}$).

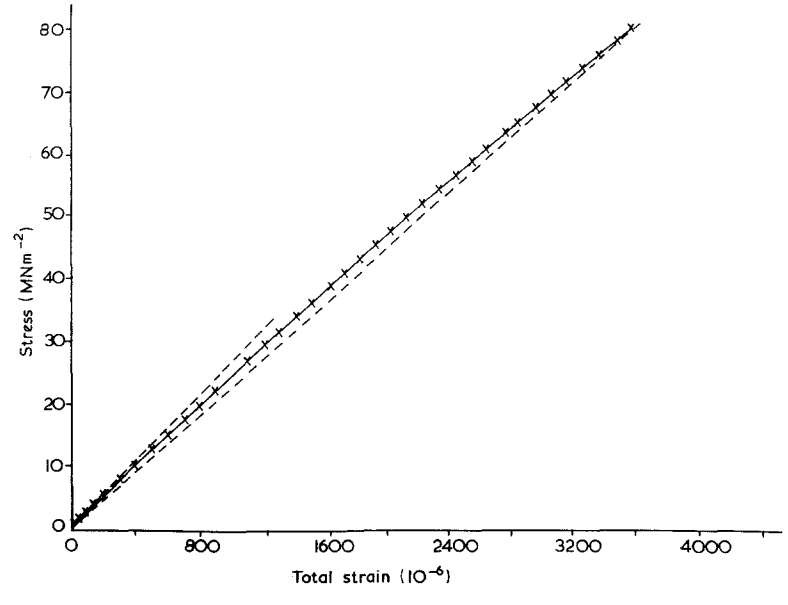

Figure 2 Typical stress–total strain behaviour to fracture, as determined with microstrain measurements (bovine femur section).

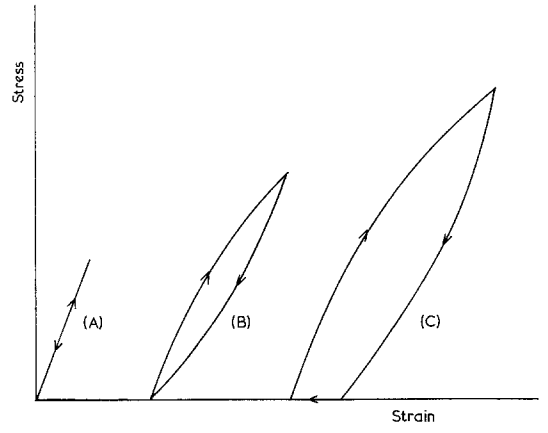

Figure 3 Schematic illustration of the three types of load–unload cycles measured with (A) a straight line (linear elastic), (B) a closed hysteresis loop (anelastic) and (C) an initially open hysteresis loop, which closes with time at zero stress (also anelastic).

The average values of Young's modulus obtained in this region for rabbit and bovine compact bone sections, were as follows:

E (rabbit tibia) = 30.8 GNm^{-2} (10 specimens)

E (rabbit femur) = 30.4 GNm^{-2} (5 specimens)

E (bovine femur) = 25.4 GNm^{-2} (21 specimens).

3.3. The transition from linear elastic behaviour

The departure from linear elastic behaviour is illustrated in Fig. 3, with a transition from a straight line load–unload cycle to a hysteresis loop (B), in which the loading and unloading curves coincided only at the maximum and zero stress (referred to as a closed hysteresis loop). At higher stress levels, the loading and unloading curves did not coincide at zero stress on unloading, giving initial residual, non-elastic strain (i.e. an open hysteresis loop), which recovered with time at zero stress to form a closed hysteresis loop (C), as illustrated in Fig. 3.

From Fig. 3, we may define the elastic limit (σ_e) as the stress above which a closed hysteresis loop is formed. This was identified by the inflexion in the stress–total strain graph or by measurement of load–unload cycles and determination of the linear line–closed loop transition.

The stress level above which an open hysteresis loop formed was identified by the measurement of residual strain at zero stress after unloading. Following previous work [4–7], this stress is designated as the microscopic yield stress (MYS) (the stress to produce a non-elastic strain of 2×10^{-6}). Direct measurement of σ_e and MYS as outlined above indicated that for all the bovine and rabbit specimens tested:

$$\sigma_e \sim \text{MYS} = 12 \pm 8\ \text{MNm}^{-2}.$$

The area of a closed hysteresis loop (ΔW) provides a measure of the energy dissipated during non-elastic deformation, while its maximum width ($\Delta\gamma$) represents the forward non-elastic strain amplitude. Hence the areas of a series of closed hysteresis loops of increasing forward non-elastic strain amplitude were measured, as shown in Figs. 4 and 5, for all the bovine and rabbit specimens, tested. The results included loops of type B and

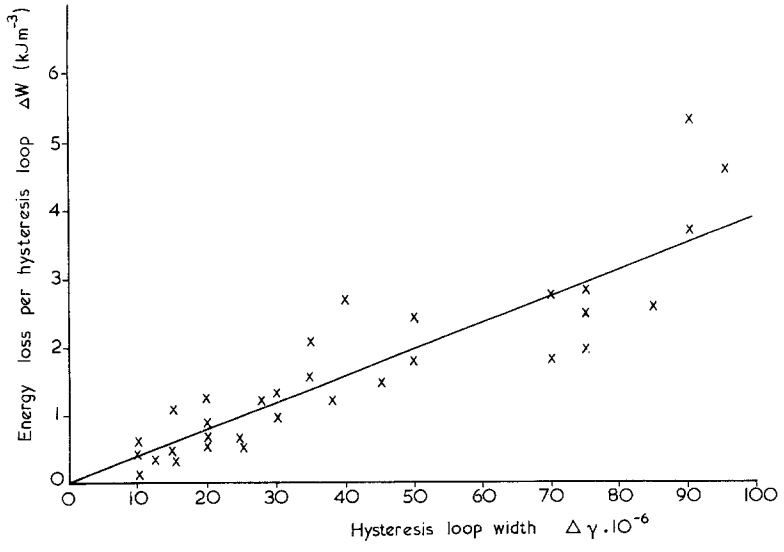

Figure 4 The variation of energy loss per hysteresis loop with forward non-elastic strain amplitude for bovine specimens.

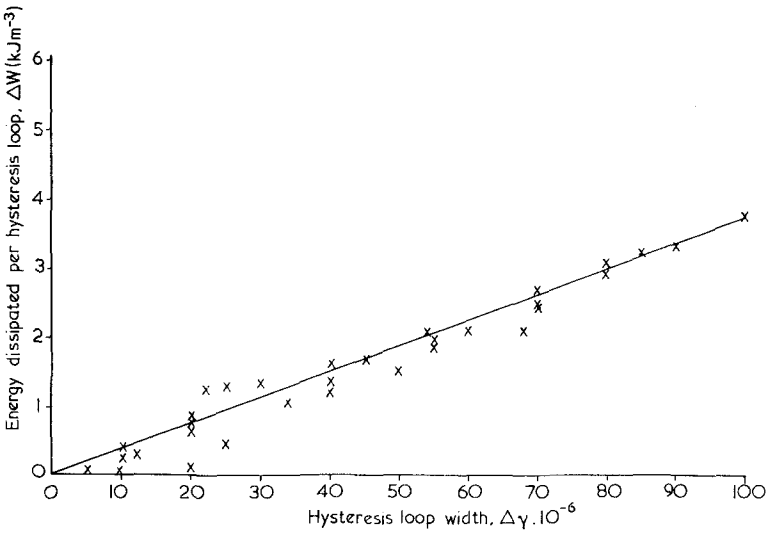

Figure 5 The variation of energy loss per hysteresis loop with forward non-elastic strain amplitude for rabbit specimens.

type C (Fig. 3). For both rabbit and bovine specimens, we obtain:

$$\Delta W = k\Delta\gamma \qquad (1)$$

where

$$k_{\text{bovine}} = 39.5\,\text{MNm}^{-2}$$

$$k_{\text{rabbit}} = 39.0\,\text{MNm}^{-2}$$

An interpretation of this data is considered in the discussion section.

3.4. Non-elastic behaviour to fracture

As the stress level was progressively increased from the MYS to fracture, there was a corresponding increase in the residual strain measured on unloading to zero stress as shown in Fig. 6. The amount of residual strain for a given stress level was dependent on the strain rate used in the load–unload cycle, as illustrated by the two rates in Fig. 6. However, in all cases, for rabbit and bovine specimens the residual strain was completely recovered with time at zero stress, as illustrated by the series

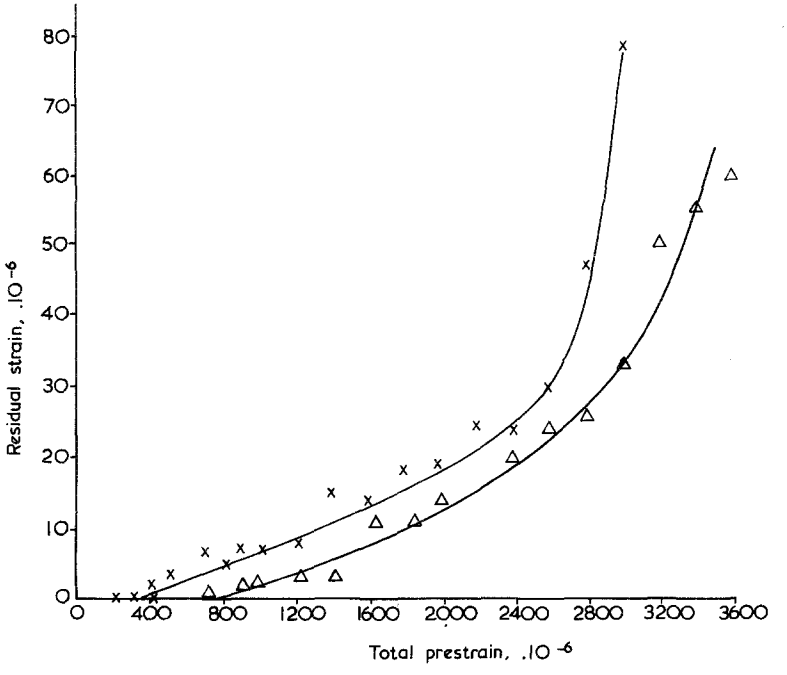

Figure 6 The residual non-elastic strain produced by various prestrains (bovine femur sections, $\dot{\epsilon} = 4.5 \times 10^{-5}$ (X), 9.0×10^{-5} (△)).

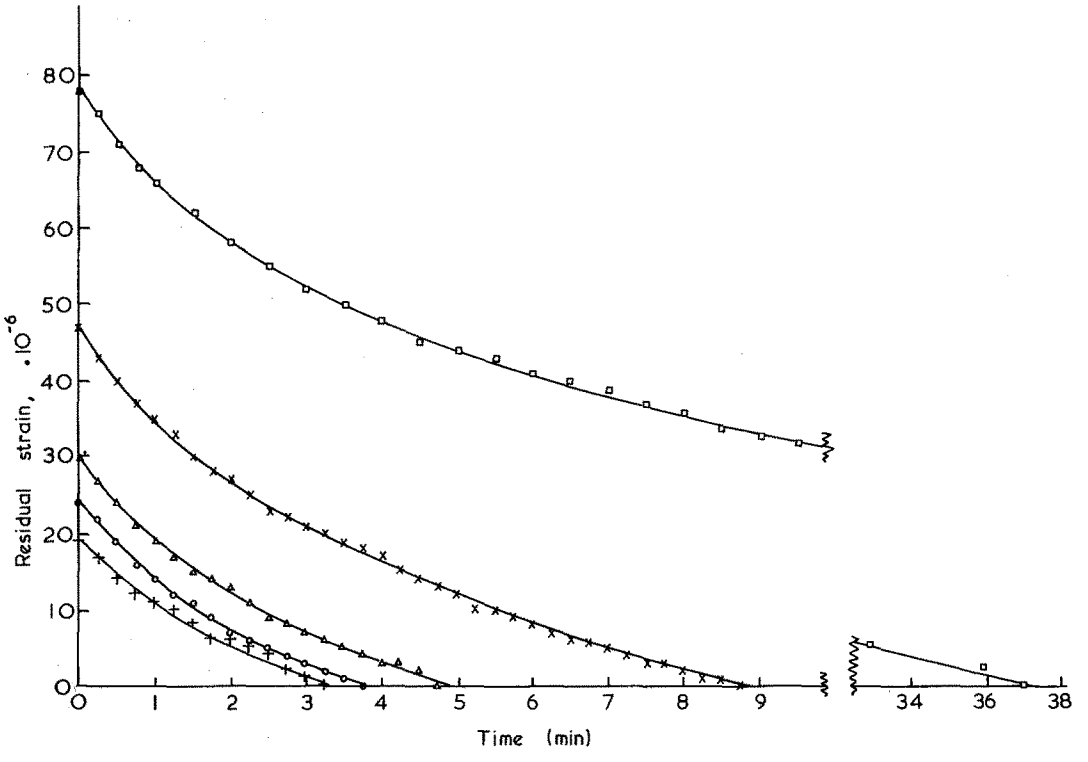

Figure 7 Recovery of residual non-elastic strain with time at zero stress following various pre-strains (bovine femur sections). (□) 3010.10^{-6}, (×) 2810.10^{-6}, (△) 2600.10^{-6}, (○) 2210.10^{-6}, (+) 2000.10^{-6}.

of curves, Fig. 7, in which the recovery of various residual strains with time at zero strain, is shown. Complete recovery of residual strain was measured for total pre-strains to $\sim 3000 \times 10^{-6}$, which represented the maximum measured strain prior to fracture.

4. Discussion

For longitudinal bovine specimens, the Young's modulus measured from the linear stress–strain region ($25.4\,GNm^{-2}$) is similar to the results of previous microstrain measurements ($26.5\,GMm^{-2}$ [7]) and ultrasonic measurements on "dry" femur sections ($26.0\,GNm^{-2}$ [9]), but is larger than the values obtained from stress–strain curves at higher levels of strain (e.g. $20.5\,GNm^{-2}$ [10], $22.7\,GNm^{-2}$ [3], $24.5\,GNm^{-2}$ [2]). The Young's modulus obtained for rabbit longitudinal sections (30.4 to $30.8\,GNm^{-2}$) is larger than that measured previously by a microstrain technique ($27.6\,GNm^{-2}$ [6]) and confirms that the difference in values between rabbit and bovine specimens is significant.

The values of MYS determined for the bovine specimens are in agreement with earlier results [4, 6], while those for rabbit sections have not been previously reported. The direct measurement results suggest that the elastic limit (σ_e) is approximately the same value as the MYS, but both values depend on the limit of the strain resolution. For this reason, the measurement of the linear dependence of energy loss in an hysteresis loop (ΔW) on forward non-elastic strain amplitude ($\Delta\gamma$) is of value. It has been demonstrated [11] that in a closed hysteresis loop, for a single deformation mechanism, then at $\Delta\gamma = 0$,

$$\Delta W = 2\sigma_F \Delta\gamma \qquad (2)$$

where σ_F (the friction stress) is the stress required for the onset of anelastic deformation. From Equation 2 and the experimental findings, Equation 1, we obtain:

$$\sigma_{F_{bovine}} = 19.8\,MNm^{-2}$$

$$\sigma_{F_{rabbit}} = 19.5\,MNm^{-2}$$

The concept of a friction stress (σ_F) for bone has not been previously advanced. It is of significance as a definition of the *onset* of anelastic de-

formation, particularly as the demonstration that the subsequent non-elastic deformation is entirely anelastic means that the MYS represents a continuation of the same physical event, rather than a measure of a second type of deformation (e.g. plastic deformation). The present data, taken from all the specimens tested, give an order of magnitude agreement between the measured values of σ_e and MYS and the derived values of σ_F, as following [11] we would expect:

$$\sigma_e\ (\sim \text{MYS}) = 2\sigma_F \qquad (3)$$

(whereas $12 \pm 8 \neq 2$ (19.5 or 19.8)). Further studies of the relationship between σ_e and σ_F on individual specimens are in progress.

After unloading from stress levels between the MYS and the ultimate tensile strength, for bovine and rabbit specimens, various amounts of residual, non-elastic strain were observed, but complete recovery of residual strain occurred with time at zero stress in all cases. Hence, it is concluded that, for these specimens, the non-elastic strain was entirely anelastic and did not contain a plastic component. The nature of deformation in reported stress–strain curves [2, 3] with relatively large non-elastic strain prior to fracture (and not obtained in the present tests) remains to be evaluated.

5. Conclusions

(1) Longitudinally oriented bovine (and rabbit) femur (and tibia) sections, deformed in tension in Ringers solution at a constant strain rate at 25° C, exhibit a limited region of elastic deformation, followed by a region of anelastic deformation.

(2) The Young's moduli of the bovine and rabbit specimens are 25.4 GNm^{-2} and 30.4 to 30.8 GNm^{-2}, respectively.

(3) For both types of the specimen, the elastic limit (σ_e) is approximately equal to the microscopic yield stress (MYS) (the stress to produce a non-elastic strain of 2×10^{-6}), with a value of $12 \pm 8\,MNm^{-2}$.

(4) Stress–strain behaviour during loading, unloading and time at zero stress, for stress increments from the MYS to fracture, follows a series of hysteresis loops, in which the energy loss (ΔW) is related to the forward non-elastic strain amplitude ($\Delta\gamma$) by:

$$\Delta W = k\Delta\gamma$$

where

$$k = 39.5\,MNm^{-2} \text{ (bovine)}$$

or

$$= 39.0\,MNm^{-2} \text{ (rabbit)}$$

The stress for the onset of anelastic strain (the friction stress, σ_F) is derived from $2\sigma_F = k$.

Acknowledgement

The authors gratefully acknowledge the provision of a research studentship (P. O'C) by the Science Research Council.

References

1. W. T. DEMPSTER and R. T. LIDDICOAT, *Am. J. Anat.* **91** (1952) 3.
2. D. REILLY, A. H. BURSTEIN and U. H. FRANKEL, *J. Biomech.* 7 (1974) 3.
3. J. D. CURREY, *ibid*, 8 (1975) 81.
4. W. BONFIELD and C. H. LI, *J. Appl. Phys.* **37** (1966) 869.
5. *Idem, J. Biomech.* 1 (1968) 323.
6. W. BONFIELD and E. A. CLARK, *J. Mater. Sci.* 8 (1973) 1590.
7. W. BONFIELD and P. K. DATTA, *J. Biomech.* 7 (1974) 147.
8. P. O'CONNOR, Ph.D. Thesis, University of London (1976).
9. S. B. LANG, *Science* **165** (1969) 287.
10. J. H. McELHANEY and E. F. BYERS, Am. Soc. Mech. Eng., Publication No. 65 – WA/HUF-9 (1965).
11. P. LUKAS and M. KLESNIL, *Phys. Stat. Solidi* **11** (1965) 127.

Received 1 May and accepted 8 June 1977.